Sensors and Actuators B 150 (2010) 806–810

Contents lists available at ScienceDirect

Sensors and Actuators B: Chemical

journal homepage: www.elsevier.com/locate/snb

Improved H_2 sensing properties of Co-doped SnO_2 nanofibers

Li Liu[a,*], Chuangchang Guo[b], Shouchun Li[a], Lianyuan Wang[a], Qiongye Dong[c], Wei Li[a]

[a] State Key Laboratory of Superhard Materials, College of Physics, Jilin University, Changchun 130012, PR China
[b] The Eleventh High School of Changchun City, Changchun 130061, PR China
[c] College of Instrumentation & Electrical Engineering, Jilin University, Changchun 130012, PR China

ARTICLE INFO

Article history:
Received 31 March 2010
Received in revised form 21 June 2010
Accepted 14 July 2010
Available online 6 August 2010

Keywords:
Electrospinning method
Nanofibers
Metal-oxide semiconductors
Gas sensors

ABSTRACT

Pure and Co-doped SnO_2 nanofibers are synthesized via an electrospinning method and characterized by X-ray diffraction (XRD), scanning electron microscopy (SEM), and transmission electron microscope (TEM). Comparing with pure SnO_2 nanofibers, Co-doped SnO_2 nanofibers exhibit improved H_2 sensing properties. Among all the samples (pure, 0.5 wt%, 1 wt%, and 3 wt% Co-doped SnO_2 nanofibers), 1 wt% Co-doped SnO_2 nanofibers show the highest response with very short response/recovery times. The response is up to 24 when the corresponding sensor is exposed to 100 ppm H_2 at 330 °C, and the response and recovery times are 2 and 3 s, respectively. Good selectivity is also observed in our investigation. These results make Co-doped SnO_2 nanofibers good candidates for fabricating high performance H_2 sensors in practical.

1. Introduction

Metal-oxide-semiconductor gas sensors have gained special focus driven by their diverse applications in air-quality detection, inflammable-gas inspection, environmental monitoring, health-care, defense, security, and so on [1–8]. Since the sensing mechanism is based on the surface reaction of these materials, their sensing performances are strongly dependent on the morphology and the structure of materials, namely, grain size, crystal system, surface area, dimension, as well as the type of grain network or porosity [9]. Recently, interest in one-dimensional (1D) nanostructures has been greatly stimulated because the sensing properties can be improved in this way [10–15].

SnO_2 is widely used for various devices, such as transparent electrodes, gas sensors, photosensors, photocatalysts, antistatic coatings, and solar cells [16]. In particular, as a gas sensor is one of its well-known applications, the synthesis of SnO_2 with particular structure or dopant can provide promising gas-sensing performances [16]. Many pure and doped SnO_2 has been exposed with high sensing characteristics. Recently, many materials, such as Zn, La, Pt, and Pd, have been proved to be effective dopants for the improvements of response or reaction speed or other characteristics of 1D SnO_2 [17–22]. However, most of these papers are focus on their ethanol sensing properties, 1D SnO_2 with high H_2 sensing properties has rarely been exposed. On the other hand, Co, which is a good dopant for many metal-oxide-semiconductors, has never been chosen for 1D SnO_2.

Here, we report the H_2 sensing properties of the Co-doped SnO_2 nanofibers synthesized via an electrospinning method. High response, quick response and recovery, and good selectivity are observed in our investigation, which indicate the potential application of Co-doped SnO_2 nanofibers for fabrication of high performance H_2 sensors.

2. Experimental

All chemicals (analytical grade reagents) were purchased from Tianjin Chemicals Co. Ltd. and used as received without further purification. Pure and Co-doped SnO_2 nanofibers were synthesized via a simple electrospinning method. Typically, an appropriate amount of $SnCl_2{\cdot}2H_2O$ was mixed with the 1:1 weight ratio of N,N-dimethylformamide (DMF) and ethanol in glove-box under vigorous stirring for 10 min. Then, this solution was in turn added into 0.8 g of poly(vinyl pyrrolidone) (PVP, Mw = 1,300,000) and the suitable amount of $Co(NO_3)_2{\cdot}6H_2O$ ($Co(NO_3)_2{\cdot}6H_2O$ and $SnCl_2{\cdot}2H_2O$ in a weight ratio of 0%, 0.5%, 1%, 3%) under vigorous stirring for 6 h. Then the mixture was loaded into a glass syringe and connected to high-voltage power supply. 10 kV was provided between the cathode (a flat aluminum foil) and anode (syringe) at a distance of 20 cm. The conversion of metal chlorides to metal oxides and the removal of PVP in as-spun nanofiber web were carried out through calcination at 600 °C for 5 h in air. Fig. 1(a) is a schematic illustration of electrospinning apparatus.

The as-synthesized sample was mixed with deionized water (resistivity = 18.0 MΩ cm^{-1}) in a weight ratio of 100:25 to form a

* Corresponding author. Tel.: +86 431 8502260.
E-mail address: liul99@jlu.edu.cn (L. Liu).

0925-4005/$ – see front matter © 2010 Elsevier B.V. All rights reserved.
doi:10.1016/j.snb.2010.07.022

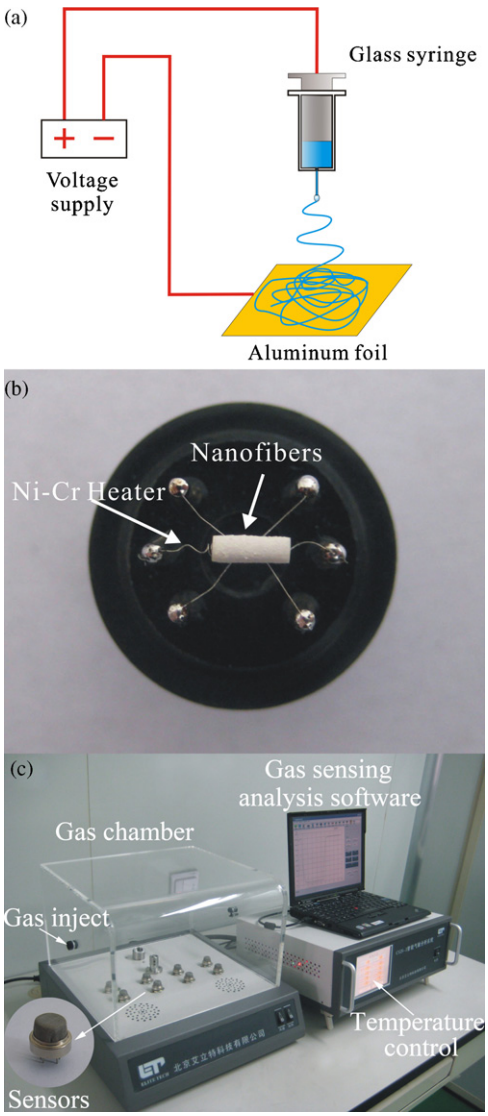

Fig. 1. (a) Schematic illustration of electrospinning apparatus, (b) a photograph of the gas sensor, and (c) a photograph of the gas-sensing analysis system.

paste. The paste was coated on a ceramic tube on which a pair of gold electrodes was previously printed, and then a Ni–Cr heating wire was inserted in the tube to form a side-heated gas sensor. A photograph of a fabricated sensor is shown in Fig. 1(b).

X-ray diffraction (XRD) analysis was conducted on a Scintag XDS-2000 X-ray diffractometer with Cu Kα radiation (λ = 1.5418 Å). Scanning electron microscopy (SEM) images were performed on a SHIMADZU SSX-550 (Japan) instrument equipped with energy dispersive X-ray (EDX) spectroscopy. Transmission electron microscope (TEM) images and selected area electron diffraction (SAED) patterns were obtained on a HITACHI S-570 microscope with an accelerating voltage of 200 kV.

Gas-sensing properties were measured by a CGS-1 intelligent gas-sensing analysis system (Beijing Elite Tech Co., Ltd, China) (Fig. 1(c)) [23]. The sensors were pre-heated at different operating temperatures for about 30 min. When the resistances of all the sensors were stable, saturated target gas was injected into the test chamber (20 L in volume) by a microinjector through a rubber plug. The saturated target gas was mixed with air (relative humidity was about 25%) by two fans in the analysis system. After the sensor resistances reached a new constant value, the test chamber was opened to recover the sensors in air. All the measurements were performed

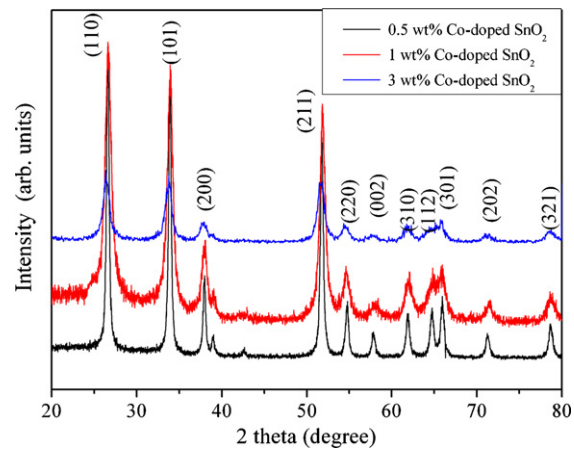

Fig. 2. XRD patterns of Co-doped SnO_2 nanofibers.

in a laboratory fume hood. The sensor resistance and response values were acquired by the analysis system automatically.

The response value (β) was defined as $\beta = R_a/R_g$, where R_a was the sensor resistance in air and R_g was a mixture of target gas and air. The time taken by the sensor to achieve 90% of the total resistance change was defined as the response time in the case of response (target gas adsorption) or the recovery time in the case of recovery (target gas desorption).

3. Results and discussion

Fig. 2 shows the XRD patterns of the Co-doped SnO_2 nanofibers. The samples are polycrystalline in nature. The prominent peaks corresponding to (1 1 0), (1 0 1) and (2 1 1) crystal lattice planes and all other smaller peaks coincide with the corresponding peaks of the rutile structure of SnO_2 given in the standard data file (JCPDS File No. 41-1445) [24].

The EDX patterns of Co-doped SnO_2 nanofibers in Fig. 3 indicate that the as-prepared nanofibers are composed of Sn, O, and Co.

Fig. 4(a) shows the SEM image of the 1 wt% PVP/Sn/Co, this precursor is highly dominated by the nanofibers with lengths of several ten micrometers and diameters ranging from 150 to 250 nm. After calcination, the diameter of the product, as shown in Fig. 4(b), is thinner than that of the precursor, indicating the removal of PVP template. The average diameter of the final product (1 wt% Co-doped SnO_2 nanofibers) is about 100 nm. Feature of an individual 1 wt% Co-doped SnO_2 nanofiber was examined by TEM (Fig. 4(c)),

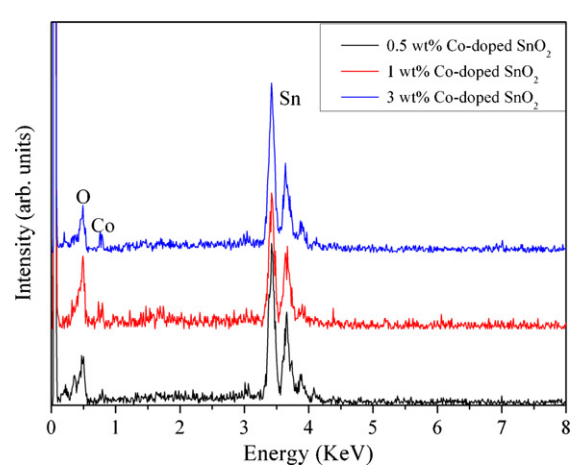

Fig. 3. EDX patterns of Co-doped SnO_2 nanofibers.

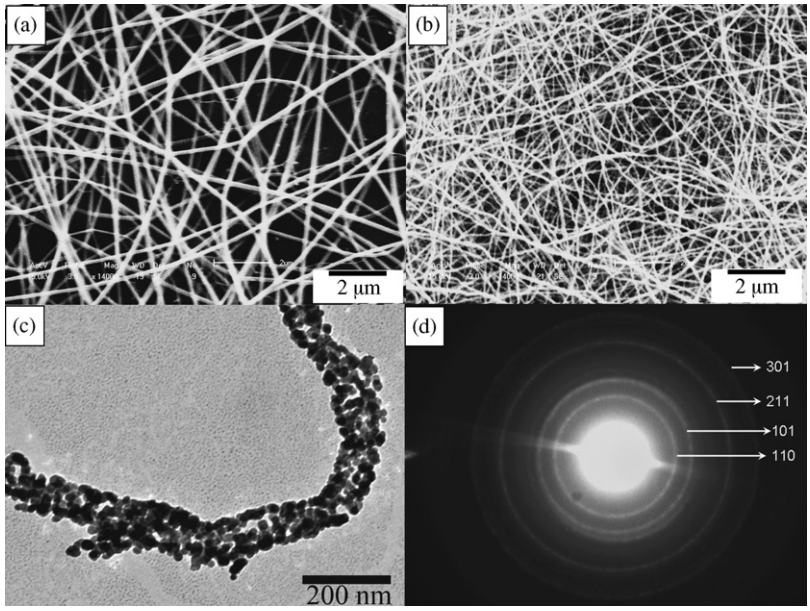

Fig. 4. (a) SEM image of 1 wt% PVP/Sn/Co, (b) SEM image of 1 wt% Co-doped SnO_2 nanofibers, (c) TEM image of 1 wt% Co-doped SnO_2 nanofibers, and (d) SAED pattern of 1 wt% Co-doped SnO_2 nanofibers.

which shows a typical characteristic of the nanofibers. The SAED pattern (Fig. 4(d)) shows that the SnO_2 nanofibers are polycrystalline in structure.

Gas-sensing experiments are performed at different operating temperatures to find the optimum operating condition. Fig. 5 shows the relationship between the different operating temperature and the response of the sensors to 100 ppm H_2. The response increases and reaches its maximum at 330 °C, and then decreased rapidly with increasing the temperature. The similar tendencies are commonly observed for all the three Co-doped SnO_2 nanofiber samples, and this behavior can be explained from the kinetics and mechanics of gas adsorption and desorption on the surface of SnO_2 or similar semiconducting metal oxides [25]. At the optimum operating temperature of 330 °C, the 1 wt% Co-doped SnO_2 sensor shows the maximum response of about 24, which is 8 times larger than that of pure SnO_2 (about 3), indicating the addition of Co is beneficial to the H_2 sensing of SnO_2 nanofibers.

Fig. 6 shows the responses of pure and Co-doped SnO_2 nanofibers to different concentrations of H_2 at 330 °C. The 1 wt% Co-doped SnO_2 nanofibers show the highest response in all the samples. The response of 1 wt% Co-doped SnO_2 nanofibers rapidly increases with the increasing H_2 concentration below 5000 ppm (the response value is about 270), and finally reaches saturation at about 25,000 ppm (the response value is about 1000).

The response versus time cures of pure and Co-doped SnO_2 nanofibers to 100 ppm H_2 are shown in Fig. 7. It can be seen that although the response value increases signally by doping Co, the response and recovery times do not change. This phenomenon suggests that doping Co may accelerate the reaction speed between SnO_2 nanofibers and H_2. The response and recovery times of 1 wt% Co-doped SnO_2 sensor are about 2 and 3 s, respectively.

The responses of 1 wt% Co-doped SnO_2 nanofibers to 100 ppm different gases are also measured at different operating temperatures (Fig. 8). The sample exhibits the highest responses to different gases at different operating temperatures. At 330 °C, this sample can successfully distinguish H_2 and these interferential gases. The response to H_2 is more than 3 times larger than that to other gases. Thus 1 wt% Co-doped SnO_2 nanofibers can be used to detect H_2 at various atmospheres.

The sensing mechanism of SnO_2 based gas sensors was clarified in previous works [1–15,26]. The most widely accepted model is that the change in resistance of the SnO_2 gas sensors is primarily

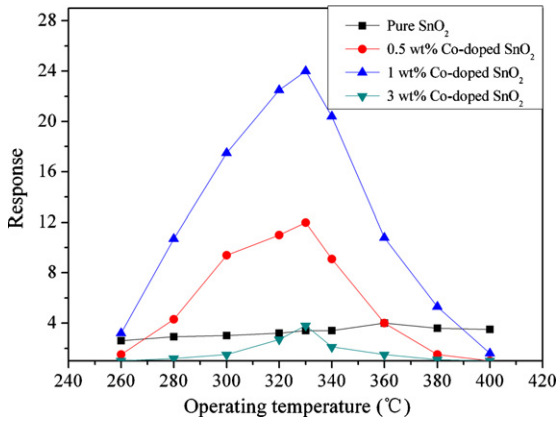

Fig. 5. Responses of pure and Co-doped SnO_2 nanofibers to 100 ppm H_2 at different operating temperatures.

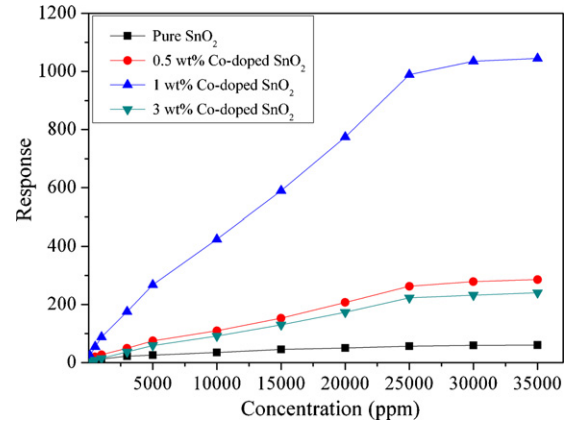

Fig. 6. Responses of pure and Co-doped SnO_2 nanofibers to different concentrations of H_2 at 330 °C.

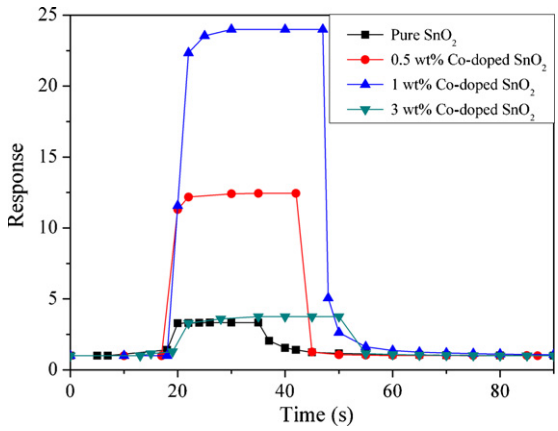

Fig. 7. Response versus time curves of pure and Co-doped SnO_2 nanofibers to 100 ppm H_2 at 330 °C.

caused by the adsorption and desorption of the gas molecules on the surface of the SnO_2 film. When SnO_2 nanofibers are exposed to air, oxygen adsorbs on the exposed surface of the SnO_2 and ionizes to O^- or O^{2-} (O^- is believed to be dominant) [27], resulting in a decrease of the carrier concentration and electron mobility. When the SnO_2 nanofibers is exposed to a reducing gas (such as H_2 in this case), the reducing gas reacts with the adsorbed oxygen molecules and releases the trapped electrons back to the conduction band, thereby increasing the carrier concentration and carrier mobility of SnO_2. Thus the resistance change of the SnO_2 sensors can be found.

Comparing with many H_2 sensors, the as-presented sensor exhibits much higher response and shorter response/recovery times, which are mainly based on the 1D structure of the nanofibers and Co doping. The large surface-to-volume ratio of 1D MOS nanostructures and the congruence of the carrier screening length with their lateral dimensions make them highly sensitive and efficient transducers of surface chemical processes into electrical signals [15]. Simultaneously, the 1D nanostructures can also avoid the aggregation growth among MOS nanoparticles [15]. Additionally, comparing with 2D nanoscale films, the interfacial areas between the active sensing region of the nanofibers and the underlying substrate are great reduced [13,15]. Those advantages lead to significant gain in high response and short response/recovery times of the as-prepared nanofibers.

Many former papers have proved that the existence of Co in MOS sensing materials can improve their sensitivity prominently [8,28–30]. The H_2 sensing improvement of in this case may be

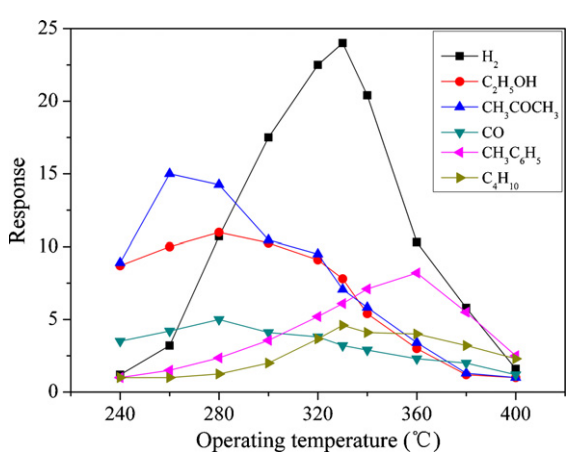

Fig. 8. Responses of 1 wt% Co-doped SnO_2 nanofibers to 100 ppm different gases.

caused by the heterocontact between the p-type Co_3O_4 and n-type SnO_2 [31,32]. The Co_3O_4 grains in SnO_2-rich materials will combine with SnO_2 electronically by forming p–n junctions, resulting in an increase in electrical resistance of the sensors. Upon exposure to H_2, the H_2 molecules can permeate into the interface of the p–n junction, lead to changes in electrical properties at the junction [33–35], and result in the large sensor response. When the Co_3O_4 content is increased too much in the sensing materials, the n-type characteristics of the materials will regress, and the n-type response (R_a/R_g) will decrease accordingly. This effect corresponds to the response fall of 3 wt% Co-doped SnO_2 nanofibers in Fig. 5.

4. Conclusion

In summary, Pure and Co-doped SnO_2 nanofibers are synthesized via an electrospinning method and their gas-sensing properties are investigated. Comparing with pure SnO_2 nanofibers, Co-doped SnO_2 nanofibers exhibit improved H_2 sensing properties. High response, short response and recovery times, and good selectivity are found based on Co-doped SnO_2 nanofibers. These gas-sensing properties are explained by the p–n junctions in Co–SnO_2 films and the 1D nanofiber structure.

Acknowledgements

This work was financially supported by the National Innovation Experiment Program for University Students (No. 2009125) and Jilin Environment Office (No. 2009-22).

References

[1] M. Lucci, A. Reale, A.D. Carlo, S. Orlanducci, E. Tamburri, M.L. Terranova, I. Davoli, C.D. Natale, A. D'Amico, R. Paolesse, Optimization of a NO_x gas sensor based on single walled carbon nanotubes, Sens. Actuators B: Chem. 118 (2006) 226–231.
[2] U. Simon, D. Sanders, J. Jockel, C. Heppel, T. Brinz, Design strategies for multielectrode arrays applicable for high-throughput impedance spectroscopy on novel gas sensor materials, J. Comb. Chem. 4 (2002) 511–515.
[3] C. Pérès, F. Begnaud, J.L. Berdagué, Standard gas addition: a calibration method for handling temporal drifts of mass spectrometry-based sensors, Anal. Chem. 74 (2002) 2279–2283.
[4] A.Z. Sadek, W. Wlodarski, K. Kalantar-Zadeh, C. Baker, R.B. Kaner, Doped and dedoped polyaniline nanofiber based conductometric hydrogen gas sensors, Sens. Actuators A: Phys. 139 (2007) 53–57.
[5] Y. Cai, A. Smith, J. Shinar, R. Shinar, Data analysis and aging in phosphorescent oxygen-based sensors, Sens. Actuators B: Chem. 146 (2010) 14–22.
[6] J.W. Jeong, Y.D. Lee, Y.M. Kim, Y.W. Park, J.H. Choi, T.H. Park, C.D. Soo, S.M. Won, I.K. Han, B.K. Ju, The response characteristics of a gas sensor based on poly-3-hexylthiophene thin-film transistors, Sens. Actuators B: Chem. 146 (2010) 40–45.
[7] A. Forleo, L. Francioso, S. Capone, P. Siciliano, P. Lommens, Z. Hens, Synthesis and gas sensing properties of ZnO quantum dots, Sens. Actuators B: Chem. 146 (2010) 40–45.
[8] K.I. Choi, H.R. Kim, K.M. Kim, D. Liu, G. Cao, J.H. Lee, C_2H_5OH sensing characteristics of various Co_3O_4 nanostructures prepared by solvothermal reaction, Sens. Actuators B: Chem. 146 (2010) 40–45.
[9] M.E. Franke, T.J. Koplin, U. Simon, Metal and metal oxide nanoparticles in chemiresistors: does the nanoscale matter? Small 2 (2006) 36–50.
[10] Y. Cui, Q. Wei, H. Park, C.M. Lieber, Nanowire nanosensors for highly sensitive and selective detection of biological and chemical species, Science 293 (2001) 1289–1292.
[11] Z.W. Pan, Z.R. Dai, Z.L. Wang, Nanobelts of semiconducting oxides, Science 291 (2001) 1947–1949.
[12] L. Durrer, T. Helbling, C. Zenger, A. Jungen, C. Stampfer, C. Hierold, SWNT growth by CVD on Ferritin-based iron catalyst nanoparticles towards CNT sensors, Sens. Actuators B: Chem. 132 (2008) 485–490.
[13] X.H. Huang, Y.K. Choi, Chemical sensors based on nanostructured materials, Sens. Actuators B: Chem. 122 (2007) 659–671.
[14] Y. Xia, P. Yang, Y. Sun, Y. Wu, B. Mayers, B. Gates, Y. Yin, F. Kim, H. Yan, One-dimensional nanostructures: synthesis, characterization, and applications, Adv. Mater. 15 (2003) 353–389.
[15] A. Kolmakov, M. Moskovits, Chemical sensing and catalysis by one-dimensional metal-oxide nanostructures, Annu. Rev. Mater. Res. 34 (2004) 151–180.
[16] L. Berry, J. Brunet, Oxygen influence on the interaction mechanisms of ozone on SnO_2 sensors, Sens. Actuators B: Chem. 129 (2008) 450–458.

[17] N.V. Hieu, H.R. Kim, B.K. Ju, J.H. Lee, Enhanced performance of SnO_2 nanowires ethanol sensor by functionalizing with La_2O_3, Sens. Actuators B: Chem. 133 (2008) 228–234.
[18] J. Hu, Y. Bando, Q. Liu, D. Golberg, Laser-ablation growth and optical properties of wide and long single-crystal SnO_2 ribbons, Adv. Funct. Mater. 13 (2003) 493–496.
[19] Q. Kuang, C. Lao, Z.L. Wang, Z. Xie, L. Zheng, High-sensitivity humidity sensor based on a single SnO_2 nanowire, J. Am. Chem. Soc. 129 (2007) 6070–6071.
[20] X.Y. Xue, Y.J. Chen, Y.G. Wang, T.H. Wang, Synthesis and ethanol sensing properties of $ZnSnO_3$ nanowires, Appl. Phys. Lett. 86 (2005) 233101/1–1233101/.
[21] Y. Zhang, X. He, J. Li, Z. Miao, F. Huang, Fabrication and ethanol-sensing properties of micro gas sensor based on electrospun SnO_2 nanofibers, Sens. Actuators B: Chem. 132 (2008) 67–73.
[22] A. Kolmakov, D.O. Klenov, Y. Lilach, S. Stemmer, M. Moskovits, Enhanced gas sensing by individual SnO_2 nanowires and nanobelts functionalized with Pd catalyst particles, Nano Lett. 5 (2005) 667–673.
[23] L. Liu, Z. Tong, L. Shouchu, W. Lianyuan, T. Yunxia, Micro-structure sensors based on ZnO microcrystals with contact-controlled ethanol sensing, Chin. Sci. Bull. 54 (2009) 4371–4375.
[24] N. Zhao, G. Wang, Y. Huang, B. Wang, B. Yao, Y. Wu, Preparation of nanowire arrays of amorphous carbon nanotube-coated single crystal SnO_2, Chem. Mater. 20 (2008) 2612–2614.
[25] N. Yamazoe, J. Fuchigami, M. Kishikawa, T. Seiyama, Interactions of tin oxide surface with O_2, H_2O and H_2, Surf. Sci. 86 (1979) 335–344.
[26] N. Barsan, D. Koziej, U. Weimar, Metal oxide-based gas sensor research: how to? Sens. Actuators B: Chem. 121 (2007) 18–35.
[27] H. Windischmann, P. Mark, A model for the operation of a thin films tin oxide conductance modulation carbon monoxide sensor, J. Electrochem. Soc. 126 (1979) 627–630.
[28] R.J. Wu, J.G. Wu, M.R. Yu, T.K. Tsai, C.T. Yeh, Promotive effect of CNT on Co_3O_4–SnO_2 in a semiconductor-type CO sensor working at room temperature, Sens. Actuators B: Chem. 131 (2008) 306–312.
[29] T. Xu, H. Huang, W. Luan, Y. Qi, S. Tu, Thermoelectric carbon monoxide sensor using Co–Ce catalyst, Sens. Actuators B: Chem. 133 (2008) 70–77.
[30] K.W. Kirby, H. Kimura, Rapid evaluation processes for candidate CO and HC sensor materials; examination of SnO_2, CO_3O_4, and $Cu_xMn_{3-x}O_4$ ($1 < x \leq 1.5$), Sens. Actuators B: Chem. 32 (1996) 49–56.
[31] U.S. Choi, G. Sakai, K. Shimanoe, N. Yamazoe, Sensing properties of SnO_2–Co_3O_4 composites to CO and H_2, Sens. Actuators B: Chem. 98 (2004) 166–173.
[32] S.B. Patil, P.P. Patil, M.A. More, Acetone vapour sensing characteristics of cobalt-doped SnO_2 thin films, Sens. Actuators B: Chem. 125 (2007) 126–130.
[33] J.D. Choi, G.M. Choi, Electrical and CO gas sensing properties of layered ZnO–CuO sensor, Sens. Actuators B: Chem. 69 (2000) 120–126.
[34] H.Y. Bae, G.M. Choi, Electrical and reducing gas sensing properties of ZnO and ZnO–CuO thin films fabricated by spin coating method, Sens. Actuators B: Chem. 55 (1999) 47–54.
[35] S.J. Jung, H. Yanagida, The characterization of a CuO/ZnO heterocontact-type gas sensor having selectivity for CO gas, Sens. Actuators B: Chem. 37 (1996) 55–60.

Biographies

Li Liu received her PhD degree in the field of microelectronics and solid state electronics in 2008 from Jilin University. She was appointed an associate professor in College of Physics, Jilin University in 2009. Now, she is interested in the field of sensing functional materials and gas sensors and humidity sensors.

Chuangchang Guo received his MS degree from the College of Physics, Jilin University, China in 2001.

Shouchun Li received his MS degree from the School of Physics and Optoelectronic Engineering, Dalian University of Technology, China in 2007.

Lianyuan Wang received her MS degree from the College of Physics, Jilin University, China in 1990.

Qiongye Dong received her MS degree from the College of Instrumentation & Electrical Engineering, Jilin University, China in 1998.

Wei Li received his MS degree from the College of Physics, Jilin University, China in 2000.